J Mater Sci: Mater Med (2010) 21:3065–3076
DOI 10.1007/s10856-010-4160-z

Anti-washout carboxymethyl chitosan modified tricalcium silicate bone cement: preparation, mechanical properties and in vitro bioactivity

Qing Lin · Xianghui Lan · Yanbao Li · Yinhui Yu · Yaru Ni · Chunhua Lu · Zhongzi Xu

Received: 9 May 2010 / Accepted: 13 September 2010 / Published online: 2 October 2010
© Springer Science+Business Media, LLC 2010

Abstract Anti-washout CaF_2 stabilized C_3S (F-C_3S) bone cement was prepared by adding water-soluble carboxymethyl chitosan (CMCS) to the hydration liquid. The setting time, compressive strength and in vitro bioactivity of the CMCS modified F-C_3S (CMCS–C_3S) pastes were evaluated. The results indicate that CMCS–C_3S pastes could be stable in the shaking simulated body fluid (SBF) after immediately mixed. The addition of CMCS significantly enhances the cohesion of particles, at the same time restrains the penetration of liquid, and thus endows the anti-washout ability. The setting times of the pastes increase with the increase of CMCS concentrations in the hydration liquid. Besides, the compressive strengths of CMCS–C_3S pastes after setting for 1–28 days are lower than that of the pure F-C_3S paste, but the sufficient strengths would be suitable for the clinical applications. The crystalline apatite deposited on the paste surface is retarded from 1 to 2 days for the addition of CMCS, but the quantities of deposited apatite are same after soaking in SBF for 3 days. As the result that pure C_3S paste has shorter setting times than pure F-C_3S paste, CMCS modified pure C_3S pastes would have better anti-washout ability. Our study provides a convenient way to use C_3S bone cement with excellent anti-washout ability when the pastes are exposed to biological fluids. The novel anti-washout CMCS–C_3S bone cement with suitable setting times, sufficient strengths and in vitro bioactivity would have good prospects for medical application.

Q. Lin · X. Lan · Y. Li (✉) · Y. Yu · Y. Ni · C. Lu · Z. Xu (✉)
State Key Laboratory of Materials-Oriented Chemical Engineering, Nanjing University of Technology, 5 Xinmofan Road, Nanjing 210009, People's Republic of China
e-mail: ybli@njut.edu.cn; lyanbao@163.com

Z. Xu
e-mail: zzxu@njut.edu.cn

1 Introduction

Tricalcium silicate (Ca_3SiO_5, C_3S), a novel self-setting biomaterial, has been shown to exhibit excellent in vitro bioactivity, bacterial leakage and biocompatibility. Actually, C_3S, the basic component of the Mineral Trioxide Aggregate (MTA), has been investigated for endodontic application since the early 1900s [1]. However, the neurotoxic aluminum ions leached from MTA may cause defects in adjacent bone growth [2, 3], and has some bad effects on biocompatibility of MTA. In addition, the complex composition of MTA makes it difficult to prepare, and its origin as well the types of preparation may affect its antimicrobial characteristics [4]. In order to avoid the disadvantages of MTA, pure C_3S has attracted the attention of many investigators for further investigation as a new bone cement [5, 6]. Several studies have proved the feasibility of pure C_3S to be used as an injectable bone-defect-filling material, as the results that pure C_3S shows good self-setting ability (hydraulic properties), excellent in vitro bioactivity, moderate degradability and cytocompatibility [5, 7–10]. Moreover, the controlled releases of biologically active Ca and Si ions from bioactive glasses lead to the upregulation and activation of seven families of genes in osteoprogenitor cells, which give rise to repaid bone regeneration [11]. Studies also have indicated that the ionic dissolution products released from pure C_3S paste in a certain concentration range also can promote the growth of osteoprogenitor cell, it suggests that Ca and Si ions are the main factors that affect the osteoprogenitor cell proliferation [12, 13]. These finding offers the possibilities of

creating a gene activating C_3S bone cement to achieve bone regeneration by controlling its ionic dissolution products [14].

However, the washout problem of C_3S bone cement may limit the further studies and potential wider applications of this novel self-setting biomaterial. The hardened C_3S paste is stable in biological fluids, but the unhardened paste would decay when it comes into contact with such fluids before the completion of the setting reaction, thus the decay of the paste would result in the failure of the operation or, at least, would decrease the effectiveness of the operation. As well as the calcium phosphate cements (CPC) [15, 16], two independent processes are thought to proceed competitively when the C_3S paste is immersed in biological fluids. One process is the polymerization and solidification of calcium silicate hydration (CSH) gel that is triggered by the hydration reaction of C_3S. Another is the penetration of liquid into the unhardened paste that induces washout of C_3S paste. Unfortunately, its initial and final setting times of 90 and 180 min with a liquid/powder (L/P) ratio of 0.8 ml/g seem too long to avoid the washout problem (Table 1). Although, $Ca(H_2PO_4)_2{\cdot}H_2O$ [17], $CaCl_2$ [18], Na_2CO_3 [19] and $CaCO_3$ [20] had been applied to reduced the setting time as shown in Table 1. The setting times of C_3S pastes with additives are also longer as compared with those of CPC [15, 21]. It is hard to avoid washout by accelerating setting process of C_3S paste. So, it is need to further develop the anti-washout C_3S bone cement by the reduction of liquid penetration.

In 1995, the no-decay CPC had been developed by employing the fast setting CPC as the based cement, and the penetration of liquid into the cement paste is reduced by the addition of sodium alginate which forms a water insoluble gel, calcium alginate. Several studies also have shown that the incorporation of a gelling agent, such as hydroxypropyl methylcellulose, carboxymethyl cellulose, alginate, chitosan, modified starch, etc., into CPC could provide good washout ability [22–24]. These admixtures improve the anti-washout ability with the respect to the cohesion of CPC by reducing bleeding, deaggregation and washout loss [22]. As it is well known, chitosan and its derivatives are useful natural biopolymers in the biomedical area due to their excellent biological properties such as biocompatibility, biodegradability, and non-toxicity properties [25, 26]. Moreover, chitosan has pharmacological benefits for bone formation [27]. With the inspiration from anti-washout CPC, carboxymethyl chitosan (CMCS) solution was applied as a hydration liquid to overcome the washout of C_3S paste.

In this study, 2 wt% CaF_2 stabilized C_3S (F-C_3S) was used, because it is more easy to prepare F-C_3S than pure C_3S as we previously described [9]. Moreover, the setting times of F-C_3S are longer than pure C_3S [5]. Such a long setting time (Table 2) is undesirable and disadvantageous to clinical application because of the cement's inability to maintain its shape and provide initial strength after surgery [21]. However, the longer setting time would be more helpful to study and evaluate the effects of CMCS on the penetration of liquid, which leads to the anti-washout and unstable of the paste before the completion of the setting reaction. In addition, the effect of CMCS solution on the compressive strength and in vitro bioactivity of F-C_3S paste were investigated.

Table 1 The setting times of pure C_3S based cements with an L/P of 0.8 ml/g at 37°C

Additives	Content (wt%)	Initial setting time (min)	Final setting time (min)	Ref.
–	–	90	180	[5]
$Ca(H_2PO4)_2{\cdot}H_2O$	20	30	90	[17]
$CaCl_2$	15	50	90	[18]
Na_2CO_3	25	20	45	[19]
$CaCO_3$	40	45	85	[20]

2 Materials and methods

2.1 Preparation of the paste

The F-C_3S used in this study was prepared by the solid state reaction as previously described [10]. Briefly, analytical reagent SiO_2, $CaCO_3$, and CaF_2 were used as starting materials and homogenized in a ceramic grinder for 12 h. Then, the raw mixtures were calcined in an electrical furnace at 1450°C, the calcined samples were removed from the furnace and quenched to room temperature in air. The calcining processes were repeated until the free lime content is lower than 0.1% (the free lime content in the sample was determined according to ASTM C114 Section 27). The F-C_3S powder was prepared by grinding the calcined sample in a ball mill for 12 h. The particle size distribution of F-C_3S powder was characterized by a flow particle analyzer (Sysemex FPIA-3000, Kobe, Japan). CMCS (carboxylation degree: 83.6%, Zhejiang Aoxing Biotechnology Co., Ltd, China) was dissolved in deionized water to form 0.50 and 1.00 wt% CMCS solutions. The viscosities of CMCS solutions were determined using a rotational viscometer (Shangping NDJ-1, Jingke, Shanghai).

To prepare the pastes, F-C_3S powder was mixed with deionized water, 0.50 and 1.00 wt% CMCS solutions with an L/P ratio of 0.67 ml/g, and named as pure F-C_3S paste, 0.50 wt% CMCS–C_3S paste and 1.00 wt% CMCS–C_3S paste (Table 2), respectively. The mixtures were mixed to form a homogeneous paste within 2 min for further experiment.

Table 2 The viscosities of hydration liquids and setting times of F-C_3S and CMCS–C_3S pastes with an L/P ratio of 0.67 ml/g at 37°C

Sample	Concentration of CMCS (wt%)	Viscosity of hydration liquid (mPa·s)	Initial setting time (min)	Final setting time (min)
Pure F-C_3S paste	0	2.50	300 ± 2	360 ± 5
0.50 wt% CMCS–C_3S paste	0.50	8.65	365 ± 2	415 ± 5
1.00 wt% CMCS–C_3S paste	1.00	17.60	430 ± 5	585 ± 7

2.2 Measurement of the setting time

The homogeneous paste was packed in the mold and put in an incubator which was kept at 37°C and 100% relative humidity. The initial (I) and final (F) setting times were measured with Vicat needle according to ISO9597-1989. The initial setting time is defined as the time elapsed between the initial contact of F-C_3S powders and hydration liquid and the time when the light needle (280 g, Ø1.13 mm) plunges into the paste and has a span of 4 ± 1 mm to the tube bottom. The final setting time is defined as the time elapsed between initial contact of F-C_3S powders and hydration liquid and the time when the heavy needle (350 g, Ø1.13 mm) no longer leaves a complete circular impression in the paste surface. The setting times were the average value of at least five specimens.

2.3 Anti-washout test

The anti-washout ability were examined by manually shaping 1.50 g homogeneous paste into a disk with the diameter of 20 mm, and then the disk was immediately soaked in 30 ml simulated body fluid (SBF, pH 7.40) in shaker with a shaking rate of 90 r/min at 37°C [28]. The SBF was prepared according to the procedure described by Kokubo [29]. The ion concentrations of the SBF were similar to those in human blood plasma. According to the reference [28], the paste was considered to pass the anti-washout ability test if it did not visibly disintegrate in SBF for 12 h.

2.4 Characterization of the paste

The homogeneous paste was molded into stainless moulds with a diameter of 10 mm and height of 18 mm, and then stored in a 37°C, 100% humidity water bath. The compressive strength was measured with a loading rate of 0.5 mm/min using a mechanical testing machine (Hualong HWT-200, Hualong, Shanghai), according to ASTM D695-91. Six replicates were carried out for each group and the result was expressed as mean ± standard deviation (mean ± SD). The phase composition and fracture section of paste curing at 37°C for 28 days were characterized by XRD (ARL XTRA, Thermo Electron, America) and SEM (JSM-6800F, JEOL, Tokyo, Japan), respectively.

2.5 Soaking in SBF

The 1-day setting pastes (Ø10 mm × 3 mm) were soaked in SBF with a surface area-to-volume ratio of 0.1 cm^{-1} and cultured in an incubator at 37°C for 7 days. The SBF was refreshed by every 12 h. Then the pastes were gently rinsed with deionized water to remove the SBF followed by drying at room temperature. The pH values of SBF after soaking with pastes for various times were measured by pH electrode (Leici pHS-2C, Jingke, Shanghai). The apatite deposited on the surface of pastes was determined by FTIR (Nexus 670, Nicolet, America) and XRD (ARL XTRA, Thermo Electron, America). The surface morphologies of pastes before and after soaked in SBF were characterized by SEM (JSM-6800F, JEOL, Tokyo, Japan).

3 Results

3.1 Characterization of F-C_3S powder

Figure 1a shows the XRD pattern of F-C_3S powder used in this study. C_3S undergoes a series of reversible phase transitions depending on temperature or impurities. There is a doublet peaks at ~52° in the XRD pattern, and the smaller peak occurs at a higher angle, these characteristics correspond to the monoclinic phase of C_3S [10]. Figure 1b shows a frequency distribution and a cumulative distribution curve of F-C_3S powder. The particle size distribution is bimodal with the peaks at about 2 and 20 μm, respectively. Cumulative percentage of particles range of 0.2–10 μm and 10–100 μm are 75.81 and 23.87%, respectively. The F-C_3S powder contains a high number of small particles.

3.2 Setting times

The viscosities of hydration liquids were determined as listed in Table 2. It is anticipated that the viscosities of hydration liquids increase with increases of the CMCS concentration. The setting times of the pastes are listed in Table 2. An increase of setting time is observed with the increase of CMCS concentration in hydration liquids. Increasing CMCS concentration from 0 to 1.00 wt% leads to a clear increase in initial setting time from 310 ± 2 to

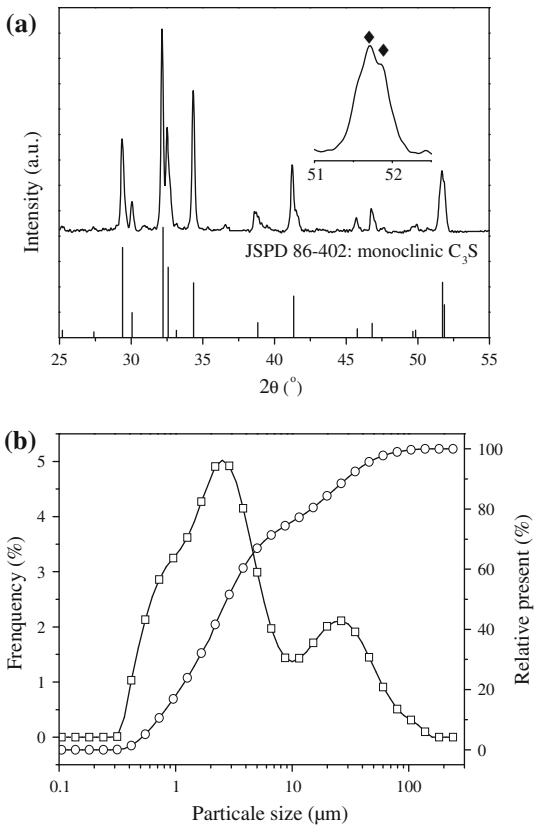

Fig. 1 XRD pattern (**a**) and particle size distribution (**b**) of F-C_3S powder

440 ± 5 min and final setting time from 370 ± 5 to 595 ± 7 min, respectively.

3.3 Anti-washout ability

Figure 2 shows the pictures of the pastes before and after immersed in the shaking SBF for 12 h. No noticeable disintegration happened for all the paste disks before immersed in SBF. Pure F-C_3S paste decays fast, and finally it is completely washed out after immersed in the shaking SBF for 12 h. CMCS–C_3S pastes do not decay obviously during shaking. Some small debris is observed on the surface of 0.50 wt% CMCS–C_3S paste, the paste disk maintains their original shape and dimension very well, and no obvious disintegration occurs. The 1.00 wt% CMCS–C_3S paste shows excellent anti-washout ability, and it remains stable in shape and sets into a hard disk without evident disintegration.

3.4 Characterization of the pastes

3.4.1 Mechanical evaluation

The compressive stress–strain curves of the pastes after curing in the water bath at 37°C for 1 day and 28 days were determined (Fig. 3). A nonlinear ascending branch before peak strength is observed in the compressive stress–strain curves of CMCS–C_3S pastes, whereas for pure F-C_3S paste, the ascending branch before peak strength almost maintains linear. The elastic modules of 1-day hardened pastes are 2547, 1628, and 1383 MPa for pure F-C_3S, 0.50 wt% CMCS–C_3S and 1.00 wt% CMCS–C_3S pastes, respectively. The elastic module of 1.00 wt% CMCS–C_3S paste is approximately 46% lower than that of pure F-C_3S paste. After setting for 28 days, the elastic modules of pure F-C_3S, 0.50 wt% CMCS–C_3S, and 1.00 wt% CMCS–C_3S pastes have increased to 3436, 2571, and 2253 MPa, respectively.

The compressive strengths of the pastes after curing in the water bath at 37°C for various times are shown in Fig. 4. It is clear to see that the compressive strengths decrease with the increase of CMCS concentration. As the result of retarded hydration by CMCS (Table 2), the 1-day compressive strengths of CMCS–C_3S pastes (23.60 ± 3.04 and 17.31 ± 1.09 MPa) are lower than that of pure F-C_3S paste (29.34 ± 3.40 MPa). The compressive strength of paste increases gradually with the time proceeding.

3.4.2 FTIR spectra

The FTIR spectra of CMCS, unhydrated F-C_3S and the 1-day setting pastes are shown in Fig. 5. In the spectrum of CMCS, the characteristic peak at 1612 cm^{-1} is attributed to the asymmetric vibration of $–COO^-$, and this suggests the existence of carboxymethyl group [30]. Furthermore, the peaks at 1414 and 1326 cm^{-1} are assigned to the symmetrical vibration of $–COO^-$ and extension vibration of C–O, respectively. Moreover, the absorption peaks at 1067 cm^{-1} shows the existence of C–O–C bond. This confirms that the –OH of chitosan has been substituted by the carboxymethyl group [30]. The absorption peaks of unhydrated C_3S at 931-889-808, 520 and 449 cm^{-1} are attributed to Si–O stretching, out of plane and in plane bending of silicate, respectively. There are not detected characteristic peaks of CMCS in the spectra of CMCS–C_3S pastes, and this may be due to the low content of CMCS in the pastes. The partially resolved doublet peak at 1430 and 1480 cm^{-1} is attributed to carbonate species for the reaction of atmospheric CO_2 with $Ca(OH)_2$ in the paste. The broad bands at 1646 and 3451 cm^{-1} arise from OH vibrations of free water in the paste matrix. The stretching mode of OH in $Ca(OH)_2$ gives rise to a sharp signal at 3643 cm^{-1} [31]. The Si–O asymmetric stretching vibration at 931 cm^{-1} in the unhydrated F-C_3S undergoes changes upon hydration. The peak at 977 cm^{-1} is attributed to the shift of the Si–O asymmetric stretching vibration in pure F-C_3S paste after setting for 1 day. The characteristic

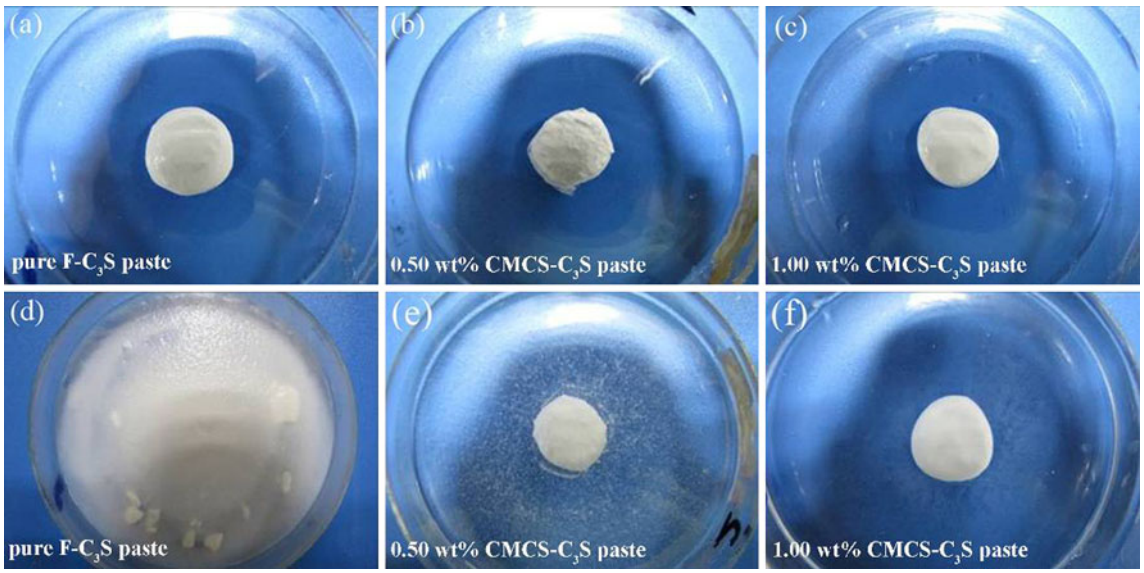

Fig. 2 Digital pictures of the pastes before (**a**, **b**, **c**) and after (**d**, **e**, **f**) immersed in the shaking SBF for 12 h

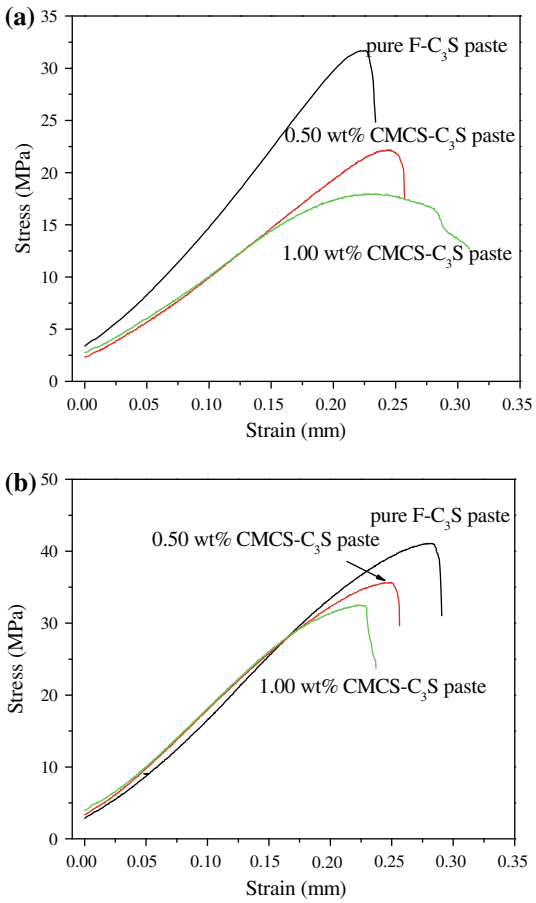

Fig. 3 Compressive stress–strain curves of the pastes after curing in the water bath at 37°C for 1 day (**a**) and 28 days (**b**)

peaks of Si–O asymmetric stretching vibration in CMCS–C_3S pastes have smaller shifts than that in pure F-C_3S paste.

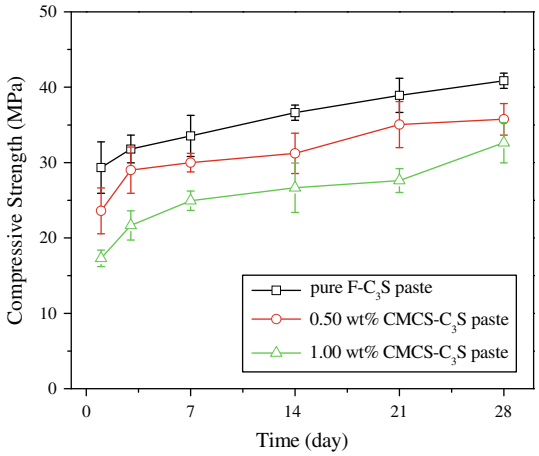

Fig. 4 Compressive strengths of the pastes after curing in the water bath at 37°C for various times

3.4.3 XRD patterns

Figure 6 shows XRD patterns of the pastes after curing in the water bath at 37°C for 28 days. After hydration for 28 days, there is a remarkable change in XRD pattern as compared with Fig. 1a, the peaks of F-C_3S are almost negligible. On the contrary, the new peak at $2\theta = 29.42°$ appears due to the formation of CSH gel, and the peaks of $Ca(OH)_2$ appears. As the result of the addition of CMCS, the peak intensity of $Ca(OH)_2$ corresponding to (001) crystal plane increases in the enlarged drawing.

3.4.4 SEM morphologies

Figure 7 illustrates SEM micrographs of the fracture sections of pastes after curing in the water bath at 37°C for

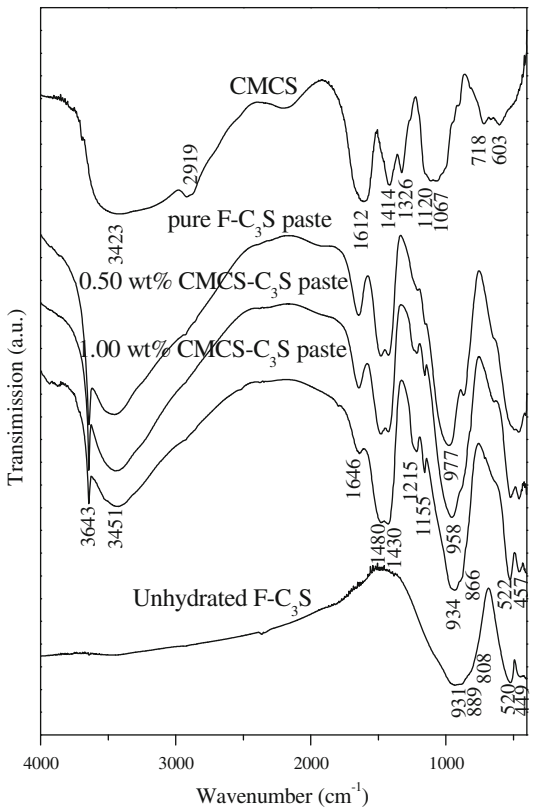

Fig. 5 FTIR spectra of CMCS, unhydrated F-C_3S and the 1-day setting pastes

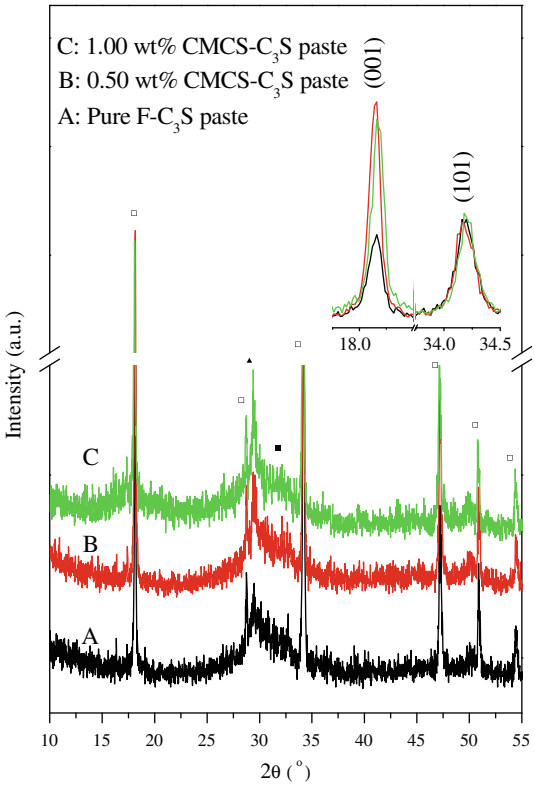

Fig. 6 XRD patterns of the pastes after curing in the water bath at 37°C for 28 days (*open square* $Ca(OH)_2$; *filled square* C_3S; *filled triangle* CSH gel)

28 days. The pastes are porous and aggregated with the needle-like crystals of CSH gel. Besides, the needle-like CSH gel in CMCS–C_3S pastes with are longer than those in pure F-C_3S paste, and the pore size in CMCS–C_3S pastes are larger.

3.5 In vitro bioactivity

3.5.1 The pH values

The pH values of SBF on the 12th hour before refreshing are presented in Fig. 8. The original pH value of SBF is 7.40. There is a quick increase of pH value after the pastes soaking in SBF for 12 h, and pure F-C_3S paste contributes to the highest pH value. As the result of prolonging soaking time from 1 to 3 days, and refreshing SBF, the pH value of SBF after soaking with paste continues to decrease. There is no obvious change of pH values after soaking for 4 days, and the pH values are very close to original pH value of SBF.

3.5.2 FTIR spectra

The FTIR spectra of the paste surfaces after soaking in SBF for various periods are shown in Fig. 9. As compared with the spectra of paste before soaking (Fig. 5), new peaks at 567 and 604 cm^{-1} in the spectra of paste after soaking in SBF are assigned to P–O bending vibration. P–O stretching vibrations give rise to a peak at 1040 cm^{-1}. The broad peak at $\sim$600 cm^{-1} is an indicator of the deposition of a layer of amorphous apatite on the surface of paste after soaking for 12 h. As the result that the amorphous apatite layer develops and transforms into crystalline phase, the band at about 600 cm^{-1} splits into double peaks (567 and 604 cm^{-1}) [32]. These splitting peaks and the peak at 1040 cm^{-1} become sharp and dominant in the FTIR spectra. It indicates that the amorphous apatite on the surface of pure F-C_3S paste, 0.50 wt% CMCS–C_3S paste and 1.00 wt% CMCS–C_3S paste develops and transforms to crystalline apatite after soaking for 1, 2 and 3 days, respectively.

3.5.3 XRD patterns

The paste surfaces after soaking in SBF for various periods were also examined by XRD (Fig. 10). The principal crystalline phases of original (1-day setting) pasts are unhydrated C_3S, CSH gel and $Ca(OH)_2$. After soaking more than 12 h, peaks corresponding to unhydrated C_3S, CSH gel and $Ca(OH)_2$ almost disappear, whereas $CaCO_3$

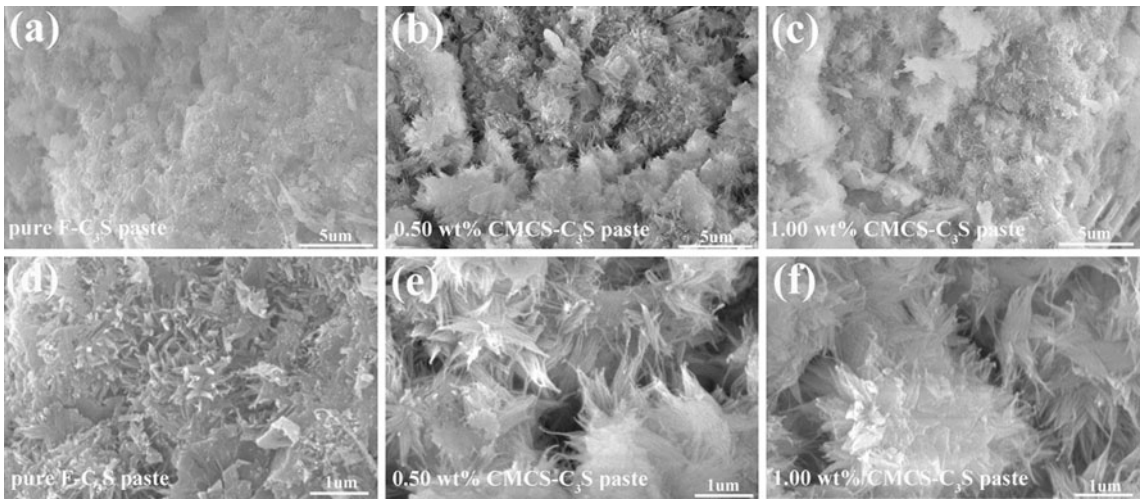

Fig. 7 SEM micrographs of the fracture sections of the pastes after curing in the water bath at 37°C for 28 days

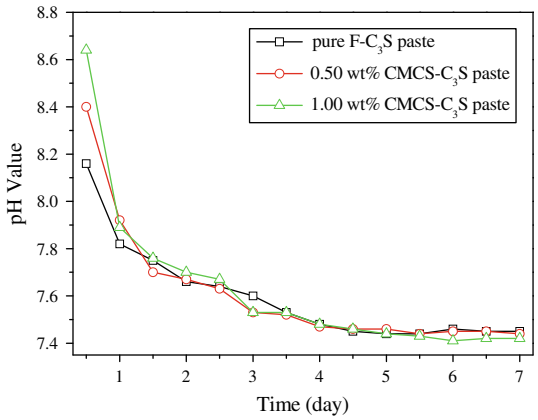

Fig. 8 pH values of SBF on the 12th hour before refreshing

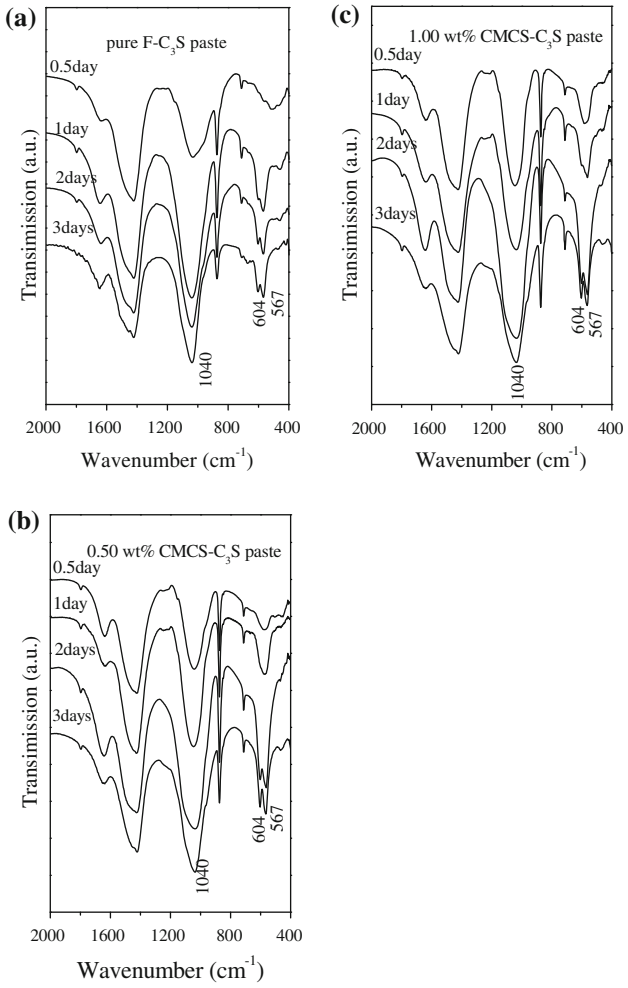

Fig. 9 FTIR spectra of the paste surfaces after soaking in SBF at 37°C for 0.5, 1, 2, and 3 days

phase appears, which is attributed to carbonization of $Ca(OH)_2$ by incorporating CO_3^{2-} from SBF [5, 31]. In addition, the peaks arising from the lower polymerization of CSH gel can also be detected in CMCS–C_3S pastes. The characteristic peaks of crystalline apatite at $2\theta = 25.90°$ and 31.96° on the surfaces of pure F-C_3S paste, 0.50 wt% CMCS–C_3S paste and 1.00 wt% CMCS–C_3S past arise after soaking for 1, 2 and 2 days, respectively. The transformation of amorphous apatite to crystalline apatite on the paste surfaces (Fig. 9) is further proved by the XRD results (Fig. 10). After immersion for 3 days, the diffraction peaks for $CaCO_3$ decrease and the characteristic peaks of crystalline apatite become the main constituent in the XRD patterns.

3.5.4 SEM morphologies

SEM micrographs of the paste surfaces before and after soaked in SBF at 37°C for various periods are shown in Fig. 11. Before soaked, the surfaces of pure F-C_3S and 0.50 wt% CMCS–C_3S pastes are compact with some micropores. The 1.00 wt% CMCS–C_3S paste is still composed of irregular C_3S particles. It suggests that the C_3S

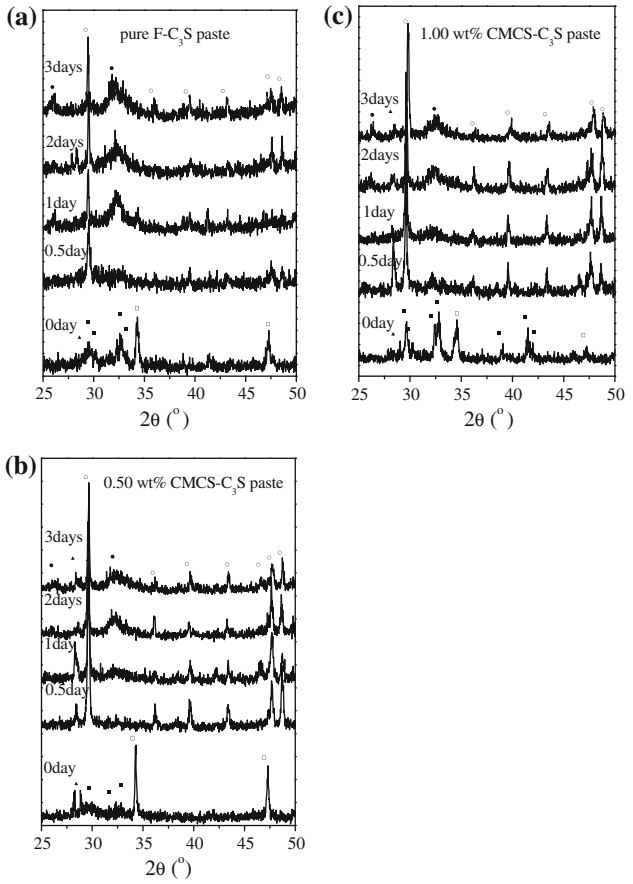

Fig. 10 XRD patterns of the paste surfaces after soaking in SBF at 37°C for 0, 0.5, 1, 2, and 3 days (*open circle* $CaCO_3$; *filled circle* apatite; *open square* $Ca(OH)_2$; *filled square* C_3S; *filled triangle* CSH gel)

particles in 1.00 wt% CMCS–C_3S paste have a lowest hydration degree than those in pure F-C_3S and 0.50 wt% CMCS–C_3S pastes. This is attributed to the retarded hydration of paste by CMCS (Table 2).

After soaking for 1 day, the micropores disappear, and tiny ball-like particles are observed on the surface of pure F-C_3S and 0.50 wt% CMCS–C_3S pastes. The higher magnification SEM micrograph shows the size of apatite particle deposited on 0.50 wt% CMCS–C_3S paste surface are lager than that on pure F-C_3S paste surface, but the amount of apatite particles on pure F-C_3S paste surface are more than that on 0.50 wt% CMCS–C_3S paste surface, and the apatite particles on pure F-C_3S paste surface are more compact. The C_3S particles of 1.00 wt% CMCS–C_3S paste aggregate, and their original shape is not visibly disintegrated after immersion for 1 day. The higher magnification SEM micrograph also shows that some tiny apatite particles have deposited on the 1.00 wt% CMCS–C_3S paste surface.

After immersion for 3 days, the apatite particles deposited on the all paste surfaces become larger and more compact. The higher magnification SEM micrographs show that the apatite particles are lath-like and agglomerate together to form an apatite layer with typical bonelike apatite morphology, and some micropores are formed on the surface again.

4 Discussion

As stated above, the major disadvantage of C_3S cement for clinical application is that it is easily decay when exposed to the biological fluids, resulting in the failure of the operation. As shown in Fig. 2d, the paste decayed completely in the absence of shaking SBF. Two opposite processes (i.e., setting and washout) take place competitively when pastes are soaked into biological fluids. It is hard to avoid washout by accelerating the setting of the paste. The main reason for the washout of paste may be the penetration of water into the paste by osmosis [23, 33, 34]. We try to restrain the penetration of liquid into the paste by addition of CMCS in the hydration liquid. To evaluate the effects of CMCS on the anti-washout ability and stable of the pastes in the shaking SBF, F-C_3S was applied for its longer setting processes as compared with pure C_3S (Tables 1 and 2) [10].

The anti-washout CMCS–C_3S pastes have been developed by addition of CMCS in the hydration liquid (Fig. 2). When F-C_3S particles react with water, a nanoporous, amorphous CSH gel forms in the original F-C_3S particles, while $Ca(OH)_2$ crystals nucleate [5]. Being free from the exposure to the biological liquids, the setting and mechanical strength of paste are attributed to the polymerization and solidification of the CSH gel. However, it is found that agglomeration of F-C_3S particles caused by the polymerization of CSH gel is hard to restrain the liquid penetration in the shaking SBF, and avoid washout before the completely setting of pure F-C_3S paste (Fig. 2d). It is considered that CMCS forms viscous solution (Table 2), and physically absorbs on the surface of F-C_3S particles, which immobilizes F-C_3S particles, and enhances agglomeration of particles, at the same time restrains the penetration of liquid into CMCS–C_3S pastes, thus endows the anti-washout ability (Fig. 2) [22]. Another possible explanation for these results (Fig. 2) may be the formation of new crosslinks by hydrogen bond and hydrophobic interaction in the CMCS–C_3S paste. As the result of the rapid increase of pH value of inner pastes to about 12.4 [5], the amino groups of CMCS would be completely deprotonated and then contributed to the loss of solubility of the chain segments and to the formation of new cross-links by hydrogen bond [35]. The immediately formation of CMCS gel may pay an important role on the improved anti-washout ability of CMCS–C_3S pastes. Additionally, the

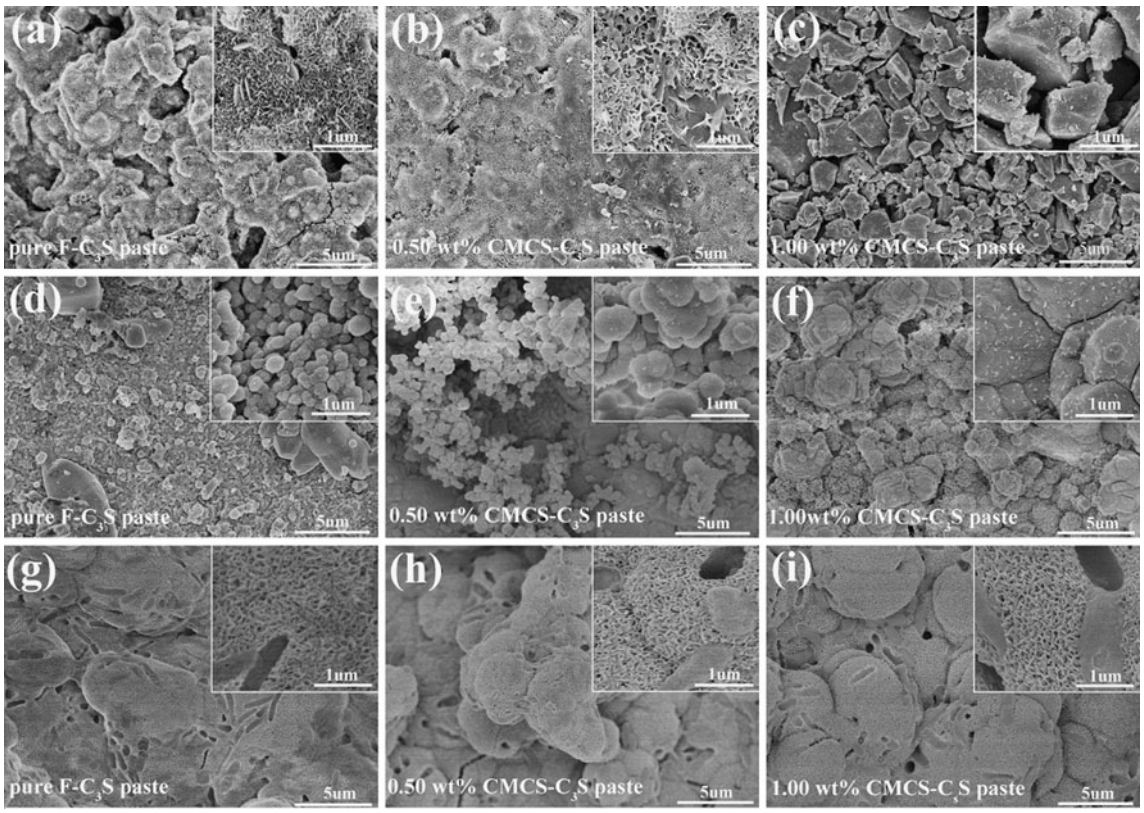

Fig. 11 SEM micrographs of the paste surfaces before soaking (**a**, **b**, **c**), after soaking in SBF at 37°C for 1 day (**d**, **e**, **f**) and 3 days (**g**, **h**, **i**)

ionic cross-links by Ca^{2+} between carboxylate ions ($–COO^-$) in CMCS and SiO_4^{4-} in CSH gel may be formed to immobilize F-C_3S particles [36]. It seems that the ionic interaction between $–COO^-$ and Ca^{2+} is too low to find direct evidence in FTIR results of CMCS–C_3S pastes (Fig. 7). However, the shifts of Si–O asymmetric stretching vibration provide of the indirect evidences. As it is well known that the shift of the Si–O asymmetric stretching vibration to a higher wavenumber is considered as the fingerprint evidence for a higher polymerization degree of CSH gel [37]. As the results of the ionic interaction between $–COO^-$ and Ca^{2+} in the CMCS–C_3S pastes, it is found that Si–O asymmetric stretching vibrations of the CMCS–C_3S pastes have smaller shifts than that of pure F-C_3S paste (Fig. 7). Furthermore, the ionic interaction between $–COO^-$ in CMCS and Ca^{2+} in $Ca(OH)_2$ results the oriented growth of $Ca(OH)_2$ in CMCS–C_3S pastes (Fig. 6).

As the time proceeding, the setting and strength of paste are attributed to the polymerization and solidification of the CSH gel. The increase of setting times with addition of CMCS (Table 2) is the consequence of CMCS absorbed on F-C_3S particles and the ionic interaction between of $–COO^-$ and Ca^{2+}, which inhibits ion diffusion and slows down the CSH gel formation, polymerization and solidification (Figs. 5, 7). For the clinical applications, the setting process of CMCS–C_3S paste could be accelerated by addition of some inorganic salts as mentioned above (Table 1). The nucleation and growth of $Ca(OH)_2$ are minimized as the results of the ionic interaction between $–COO^-$ and Ca^{2+} [36], and the crystalline $Ca(OH)_2$ in CMCS–C_3S pastes grows along (001) crystal plane (Fig. 6). Although, the longer needle-like CSH gel in CMCS–C_3S pastes is observed (Fig. 7), bigger and more pores are observed in the CMCS–C_3S paste (Fig. 7). CMCS does not increase the interlocking of CSH gel for the compressive strengths, and thus can be taken just as an impurity form the interlocking reaction. Thus, the 1-day compressive strengths of the pastes are obviously decreased with the addition of CMCS (Figs. 3, 4), but the compressive strengths are tolerable and higher than that of cancellous bone (5–10 MPa) [38], which could enable to attain the necessary initial strength for the graft. It is worthy to note that the 1-day elastic modules of the CMCS–C_3S pastes are decreased obviously (Fig. 3), the low elastic modules of CMCS–C_3S pastes are more compatible to that of bone, and maybe beneficial for the loading condition. The lower strengths of the CMCS–C_3S pastes (Fig. 4) are attributed to their higher porosity (Fig. 7). Besides, the final compressive strengths (28 days) of the CMCS–C_3S pastes are more than 30 MPa, this value is valuable for the fabrication bone substitute materials [38].

The apatite formation ability is an essential property for C_3S paste, and this apatite layer can reproduce in vitro by soaking in SBF with ion concentrations nearly equal to those in human blood plasma. The effect of CMCS on the apatite formation ability was evaluated by pH value, FTIR, XRD and SEM. As the results of the slowing down hydration of F-C_3S with the addition of CMCS, the initial pH values of SBF soaking with CMCS–C_3S pastes are lower than that soaking with pure F-C_3S paste (Fig. 8). After the pastes soaking in dynamic SBF, the subsequent pH values of soaking environment decrease to about 7.40 (Fig. 8), which is opposite to previous studies soaking in a static SBF [5]. The transformation of $Ca(OH)_2$ into $CaCO_3$ and the deposition of apatite contribute to the continuous decreasing of pH values (Fig. 8). It is believed that this dynamic condition leads to a more precise in vitro study, and is more similar to the body environment [39]. Interestingly, amorphous apatite deposited on pure F-C_3S and CMCS–C_3S paste surfaces have been observed after soaking for 12 h (Figs. 9, 11). Meanwhile, the hydration-derived $Ca(OH)_2$ reacts with HCO_3^- in SBF and transforms into $CaCO_3$ (Fig. 10), which also have the good biocompatibility and bond adaption [40]. The outstandingly efficient deposition of apatite on paste surface is attributed to the rapid dissolution of $Ca(OH)_2$ and the high proportion of pre-existing Si–OH nucleation site presented by the nanoporous CSH gel structure (Fig. 9). However, the transformation time of the amorphous apatite to crystalline apatite on the paste surfaces has been prolongs form 1 day to 2 days as the result of the addition of CMCS (Fig. 9, 10). It could be explained that the ion exchanges between SBF and CMCS–C_3S pastes are lowed by the inhibitory effect of CMCS. From a more quantitative point of view, a quantitative analysis of apatite layer after soaking in SBF is determined by SEM to complement the findings to understand deposition ability of apatite. Although, there are more apatite particles deposited on the surface of pure F-C_3S paste than on CMCS–C_3S paste surfaces after soaking in SBF for 1 day. The apatite layers deposited on their surfaces are similar after soaking in SBF for 3 days. Therefore, it is concluded that the level of in vitro bioactivity of CMCS–C_3S pastes is lower than that of pure F-C_3S pastes, but the quantity of deposited apatite are same after soaking for 3 days.

In this study, F-C_3S was used to investigate the anti-washout ability. Pure C_3S paste has shorter setting times than pure F-C_3S paste, and the shorter setting time would results the weaker effect of the liquid penetration. In practice, CMCS modified pure C_3S pastes would show better anti-washout ability. Originally, fabrication of anti-washout CPC was achieved by using chitosan solution as hydration liquid [41]. It has been reported that chitosan forms a water-insoluble gel, and produces a reductive effect on the fluid penetration process which was the cause of decay [41]. Therefore, it is concluded that the mechanism of anti-washout behavior is, at least in part, reduction of fluid penetration into the paste. Gelatin is a candidate additive capable of forming a water-insoluble gel, and the anti-washout ability of calcium silicate cement has been improved with the addition of gelatin. However, CMCS has a less inhibitory effect on the setting reaction than gelatin [42]. For example, the addition of gelatin significantly prolonged the setting times of calcium silicate cements by about 2–8 times [42]. As compared with gelatin, CMCS maybe a superior additive to prepare the anti-washout calcium silicate and C_3S based cements.

Washout is a key problem of pure C_3S paste when it may be exposed to the biological fluids, because washout would make the paste fail to set and provide the strength to support the bone defects. CMCS–C_3S pastes with the excellent anti-washout ability, suitable setting times, sufficient strengths and in vitro bioactivity would avoid the failure of the operation in the above situations. Anti-washout CMCS–C_3S pastes could be wider and safer applied in biomedical fields including orthopaedics, plastic and reconstructive surgery, and oral and maxillofacial surgery. According to the requirements of the non-decay/anti-washout cement sated by Iskikawa et al. [15], the handing properties and biocompatibility of CMCS–C_3S pastes are need to evaluated or further improved. For better handing properties in term of the clinical applications, smaller amount of additive is desirable to accelerate the setting process of CMCS–C_3S paste. Although the synergistic combination of chitosan and CPC has shown a better tissue response than pure CPC [41, 43], more studies need to be conducted on the biocompatibility of CMCS–C_3S cements.

5 Conclusions

The anti-washout CMCS–C_3S pastes were developed by adding CMCS to hydration liquid with an L/P ratio of 0.67 ml/g. CMCS–C_3S pastes could be stable in the shaking SBF after immediately mixed. The addition of CMCS significantly enhances the cohesion of F-C_3S particles, at the same time restrains the penetration of liquid, and thus endows the anti-washout ability. The setting times of the pastes increase with the increase of CMCS concentrations in the hydration liquid. Besides, the compressive strengths of CMCS–C_3S paste after setting for 1–28 days are lower than that of the pure F-C_3S paste, but the sufficient mechanical strength would be suitable for the clinical applications. The crystalline apatite deposited on the paste surface is retarded from 1 to 2 days for the addition of CMCS, but the quantities of deposited apatite are same

after soaking in SBF for 3 days. As the result that pure C_3S paste has shorter setting times than pure F-C_3S paste, CMCS modified pure C_3S would have better anti-washout ability. Novel anti-washout ability CMCS–C_3S pastes with suitable setting times, sufficient strengths and in vitro bioactivity could have good prospects for biomedical application.

Acknowledgments This work is financially supported by the National Basic Research Program of China (973 Program) (2009CB623105), National Natural Science Foundation of China (50802042), Natural Science Foundation of Jiangsu province, China (BK2008379), Science and Technology Developing Foundation of Nanjing (ZKX07016), State Key Laboratory of Materials-Oriented Chemical Engineering (KL09-6) and Graduate Innovation Foundation of Jiangsu Province (CX09B-127Z).

References

1. Roberts HW, Toth JM, Berzins DW, Charlton DG. Mineral trioxide aggregate material use in endodontic treatment: a review of the literature. Dent Mater. 2008;24(2):149–64.
2. Exley C. A molecular mechanism of aluminium-induced Alzheimer's disease? J Inorg Biochem. 1999;76(2):133–40.
3. Brook IM, Hatton PV. Glass-ionomers: bioactive implant materials. Biomaterials. 1998;19(6):565–71.
4. Al-Hezaimi K, Al-Shalan TA, Naghshbandi J, Simon JHS, Rotstein I. MTA preparations from different origins may vary in their antimicrobial activity. Oral Surg Oral Med Oral Pathol Oral Radiol Endod. 2009;107(5):e85–8.
5. Zhao W, Wang J, Zhai W, Wang Z, Chang J. The self-setting properties and in vitro bioactivity of tricalcium silicate. Biomaterials. 2005;26(31):6113–21.
6. Zhao W, Chang J. Two-step precipitation preparation and self-setting properties of tricalcium silicate. Mater Sci Eng. 2007; 28(2):289–93.
7. Zhao W, Chang J. Sol-gel synthesis and in vitro bioactivity of tricalcium silicate powders. Mater Lett. 2004;58(19):2350–3.
8. Zhao W, Chang J, Wang J, Zhai W, Wang Z. In vitro bioactivity of novel tricalcium silicate ceramics. J Mater Sci Mater Med. 2007;18(5):917–23.
9. Lin Q, Li Y, Lan X, Lu C, Chen Y, Xu Z. The apatite formation ability of CaF_2 doping tricalcium silicates in simulated body fluid. Biomed Mater. 2009;4:045005.
10. Lin Q, Li Y, Lan X, Lu C, Xu Z. The Effect of CaF_2 on the preparation and in vitro bioactivity of tricalcium silicates. Chin J Inorg Chem. 2008;24(12):1937–42.
11. Christodoulou I, Buttery LD, Saravanapavan P, Tai G, Hench LL, Polak JM. Dose- and time-dependent effect of bioactive gel-glass ionic-dissolution products on human fetal osteoblast-specific gene expression. J Biomed Mater Res B Appl Biomater. 2005;74B(1):529–37.
12. Laurent P, Camps J, De Meo M, Dejou J, About I. Induction of specific cell responses to a Ca_3SiO_5-based posterior restorative material. Dent Mater. 2008;24(11):1486–94.
13. Gandolfi MG, Pagani S, Perut F, Ciapetti G, Baldini N, Mongiorgi R, Prati C. Innovative silicate-based cements for endodontics: a study of osteoblast-like cell response. J Biomed Mater Res. 2008;87A(2):477–86.
14. Hench LL. Genetic design of bioactive glass. J Eur Ceram Soc. 2008;29(7):1257–65.
15. Ishikawa K, Miyamoto Y, Kon M, Nagayama M, Asaoka K. Non-decay type fast-setting calcium phosphate cement: composite with sodium alginate. Biomaterials. 1995;16(7):527–32.
16. Kai D, Li D, Zhu X, Zhang L, Fan H, Zhang X. Addition of sodium hyaluronate and the effect on performance of the injectable calcium phosphate cement. J Mater Sci Mater Med. 2009; 20(8):1595–602.
17. Zhiguang Huan JC. Novel tricalcium silicate/monocalcium phosphate monohydrate composite bone cement. J Biomed Mater Res. 2007;82B:352–9.
18. Wang X, Sun H, Chang J. Characterization of Ca_3SiO_5/$CaCl_2$ composite cement for dental application. Dent Mater. 2008; 24(1):74–82.
19. Huan Z, Chang J. Effect of sodium carbonate solution on self-setting properties of tricalcium silicate bone cement. J Biomater Appl. 2008;23(3):247–62.
20. Huan Z, Chang J. Study on physicochemical properties and in vitro bioactivity of tricalcium silicate-calcium carbonate composite bone cement. J Mater Sci Mater Med. 2008;19(8):2913–8.
21. Kunio I, Miyamoto Y, Takechi M. Non-decay type fast-setting calcium phosphate cement: hydroxyapatite putty containing an increased amount of sodium alginate. J Biomed Mater Res. 1997;36(3):393–9.
22. Xiupeng W, Ling C, Hong X, Jiandong Y. Influence of anti-washout agents on the rheological properties and injectability of a calcium phosphate cement. J Biomed Mater Res. 2007; 81B(2):410–8.
23. Takagi S, Chow LC, Hirayama S, Eichmiller FC. Properties of elastomeric calcium phosphate cement-chitosan composites. Dent Mater. 2003;19(8):797–804.
24. Cherng A, Takagi S, Chow LC. Effects of hydroxypropyl methylcellulose and other gelling agents on the handling properties of calcium phosphate cement. J Biomed Mater Res. 1997;35(3):273–7.
25. Shirosaki Y, Tsuru K, Hayakawa S, Osaka A, Lopes MA, Santos JD, Costa MA, et al. Physical, chemical and in vitro biological profile of chitosan hybrid membrane as a function of organosiloxane concentration. Acta Biomater. 2009;5(1):346–55.
26. Lee EJ, Shin DS, Kim HE, Kim HW, Koh YH, Jang JH. Membrane of hybrid chitosan-silica xerogel for guided bone regeneration. Biomaterials. 2009;30(5):743–50.
27. Muzzarelli RAA, Mattioli-Belmonte M, Tietz C, Biagini R, Ferioli G, Brunelli MA, Fini M, et al. Stimulatory effect on bone formation exerted by a modified chitosan. Biomaterials. 1994;15(13):1075–81.
28. Kokubo T, Takadama H. How useful is SBF in predicting in vivo bone bioactivity? Biomaterials. 2006;27(15):2907–15.
29. Shozo T, Laurence CC, Satoshi H, Akiyoshi S. Premixed calcium-phosphate cement pastes. J Biomed Mater Res. 2003; 67B(2):689–96.
30. Lin Y, Chen Q, Luo H. Preparation and characterization of N-(2-carboxybenzyl)chitosan as a potential pH-sensitive hydrogel for drug delivery. Carbohydr Res. 2007;342(1):87–95.
31. Coleman NJ, Awosanya K, Nicholson JW. Aspects of the in vitro bioactivity of hydraulic calcium (alumino) silicate cement. J Biom Mater Res. 2008;90 A(1):166–74.
32. Peitl O, Dutra Zanotto E, Hench LL. Highly bioactive P_2O_5–Na_2O–CaO–SiO_2 glass-ceramics. J Non-Crystal Solids. 2001;292(1–3):115–26.
33. Wang X, Ma J, Wang Y, He B. Structural characterization of phosphorylated chitosan and their applications as effective additives of calcium phosphate cements. Biomaterials. 2001; 22(16):2247–55.
34. Rau JV, Generosi A, Smirnov VV, Ferro D, Rossi Albertini V, Barinov SM. Energy dispersive X-ray diffraction study of phase development during hardening of calcium phosphate bone

cements with addition of chitosan. Acta Biomater. 2008; 4(4):1089–94.
35. Chen L, Tian Z, Du Y. Synthesis and pH sensitivity of carboxymethyl chitosan-based polyampholyte hydrogels for protein carrier matrices. Biomaterials. 2004;25(17):3725–32.
36. Lin YH, Liang HF, Chung CK, Chen MC, Sung HW. Physically crosslinked alginate/N, O-carboxymethyl chitosan hydrogels with calcium for oral delivery of protein drugs. Biomaterials. 2005; 26(14):2105–13.
37. Mollah MYA, Yu W, Schennach R, Cocke DL. A Fourier transform infrared spectroscopic investigation of the early hydration of Portland cement and the influence of sodium lignosulfonate. Cem Con Res. 2000;30(2):267–73.
38. O'Kelly K, Tancred D, McCormack B, Carr A. A quantitative technique for comparing synthetic porous hydroxyapatite structures and cancellous bone. J Mater Sci: Mater Med. 1996;7(4): 207–13.
39. Ramila A, Vallet-Regi M. Static and dynamic in vitro study of a sol-gel glass bioactivity. Biomaterials. 2001;22(16):2301–6.
40. Yoshitsugu F, Takao Y, Takashi N, Seiya K, Chikara O, Tadashi K. The bonding behavior of calcite to bone. J Biomed Mater Res. 1991;25(8):991–1003.
41. Takechi M, Miyamoto Y, Ishikawa K, Yuasa M, Nagayama M, Kon M, Asaoka K. Non-decay type fast-setting calcium phosphate cement using chitosan. J Mater Sci Mater Med. 1996;7(6):317–22.
42. Chen CC, Lai MH, Wang WC, Ding SJ. Properties of anti-washout-type calcium silicate bone cements containing gelatin. J Mater Sci Mater Med. 2010;21(4):1057–68.
43. Takechi M, Miyamoto Y, Ishikawa K, Toh T, Yuasa T, Nagayama M, Suzuki K. Initial histological evaluation of anti-washout type fast-setting calcium phosphate cement following subcutaneous implantation. Biomaterials. 1998;19(22):2057–63.